JET–R(97)17

A Preliminary Analysis of a Global Energy Confinement Database for JET Deuterium Ohmic Plasma from 1994, 1995 and 1996 Campaigns

G Bracco[1], K Thomsen.

JET Joint Undertaking, Abingdon, Oxfordshire, OX14 3EA,

[1] Associazione EURATOM-ENEA sulla Fusione, Centro Richerche Energia Frascati, C.P. 65-00044 Frascati (Rome), Italy.

December 1997

ABSTRACT.

A database containing global energy confinement data for JET ohmic plasmas from the campaigns 1994-96 has been established. This paper presents an anlysis of this database for the JET tokamak with the Mark I and II divertors and compares the results with the data from the 1984-92 campaigns.

I. INTRODUCTION

The global energy confinement for JET ohmic plasma has been recently examined in a paper [1] devoted to the analysis of the results obtained in the campaigns from 1984 to 1992, before the introduction of the JET pumped divertor. The present work is dedicated to the analysis of the ohmic results from the experimental campaigns performed in the years 1994 and 1995, during the MARK I divertor operation, and from most of the 1996 campaign, after the divertor modification to MARK II configuration.

As in the previous work, the aim is to assess the global energy confinement behaviour for standard JET ohmic plasma. A database containing data for ohmic heated plasma in stationary conditions has been constructed, by selecting a subset of the JET transport database, and a detailed analysis has been performed. In section 2 the selection criteria are described and in section 3 the resulting database is described and analysed. Section 4 is dedicated to the comparison of the results with the global energy confinement scaling laws. In section 5 the magnetic field dependence of the global energy confinement time in the saturated ohmic regime is discussed. Section 6 performs a comparison of the present results with the ohmic data from JET previous campaigns. Finally the conclusions are drawn in section 7.

II. DATA SELECTION CRITERIA

The database used in the previous work [1] was constructed on the basis of a pre-selection of significant ohmic data time points, that had been established during the years of operations 1984 to 1992. This pre-selection was not available for the data of the years 1994 to 1996 so an equivalent, somewhat automatic, selection procedure had to be implemented. The selection criteria applied in the previous work [1], also had to be adapted to match the present status of the JET data in order to construct the ohmic database analysed in this paper.

The JET transport database for the concerned years (from 1994 up to the end of November 1996) consists of about 240000 time slices, 127000 without or with negligible (<5%) additional heating (6700 pulses). We restrict our attention to the subset consisting of pure ohmic pulses for a total of 26000 observations, 23000 of which are from Deuterium plasmas, while most of the remaining 3000 time slices refer to gas mixtures. If only the time slices during the current flat top are retained the Deuterium subset is reduced to 10790 observations, for a total of 965 differ-

ent pulses. By excluding data for which the plasma configuration is not readily available the selection is reduced to 9361 observations from 831 pulses. The diverted plasma data account for 5118 time slices in this subset.

The next step in selection procedure requires the availability of the main confinement data. In the previous work [1] the global energy confinement time τ_E has been estimated from the plasma kinetic energy content W_{kin}, as determined from the measured electron temperature (ECE emission), the electron density (DCN interferometer) and the ion temperature deduced from the neutron yield monitors. By applying the same approach, the following plasma data have been required: plasma current I_P, toroidal magnetic field B_T, ohmic power P_{OH}, volume averaged electron density <n> from the DCN interferometer, peak electron temperature T_{e0} from ECE emission. It is also required that $0.1 < T_{e0} < 10$ keV and $0.1 < \langle n \rangle < 10\ 10^{19}\ m^{-3}$. The last time slice of each pulse is rejected as it is often at the very end of the current flat top. These constraints reduce the subset to 4736 observations.

The following step involves the identification of some constraints to identify the time slices during plasma stationary conditions: it has been chosen to evaluate the values of the average μ and standard deviation σ for each group of subsequent 3 time slices in the same pulse, for some of the key quantities I_P, B_T, <n>, the safety factor q_{cyl}, the elongation k, and to require the relative deviation σ/μ to be lower than a given threshold. A fixed acceptance range has been assigned also for d_t, defined as the time interval between the first and the last time slice of each group of 3 time slices. The thresholds have been set in a somewhat arbitrary way, using as a reference the average value of σ/μ on the given data subset of 4736 observations. Table 1 shows the average values, the threshold values and the number of rejected time slices.

Table 1. Selection criteria for stationary conditions.

Data	**Average of σ/μ**	**Threshold values**	**Rejected cases**
IP	0.8 %	> 4 %	1
BT	1.3 %	> 3 %	244
<n>	7.4 %	> 5 %	1476
qcyl	2.3 %	> 4 %	495
k	0.8 %	> 2 %	562
dt	1.9 s (absolute)	< 1 s	143
		> 3 s	14

The acceptance range for the time interval d_t has been chosen so that at least 1 s of stationary conditions can be identified, and the condition d_t not greater than 3 s prevents the average of rather unrelated time slices. The minimum $d_t = 1$ s is also connected with the necessity of

recomputing the time average of the loop voltage V_{sur} in order to minimise the effect of the its large time oscillations on the evaluation of the ohmic power [1].

The selection criteria from Table 1 reduce the database to 1801 time slices, some of which are overlapping in time. By selecting only non-overlapping times slices a subset of 900 observations, from 450 different pulses has been created. In the selection of non-overlapping time slices, later times in the discharges have been preferred as the current density profile at later times should be nearer to the relaxed stationary case.

At this point of the data selection, the time traces of I_P, B_T, <n> and V_{sur} for each of the selected pulses have been plotted and checked. Some of the time slices have been rejected while others have been shifted to a different time slice available in the transport database. This procedure results in a database of 776 observations. As in [1] the values of V_{sur}, the loop voltage on plasma axis V_{axis} and the ohmic power P_{OH} have been recomputed by averaging on a 1 s time interval.

Other considerations can be drawn from the observation of the time traces. Often the data in the limiter configuration in the first phase of the current flat top are taken during a ramp of B_T and this situation has been marked with a flag in the database. The value of <n> as measured by the DCN interferometer is often affected by uncorrected fringe jumps. All the cases that have been spotted have been marked by a corresponding flag in the database, but the accuracy of the value of <n> from the DCN interferometer can not be assured, at least without a detailed check of the full set of the interferometer data for each pulse.

The latter problem has required a dedicated approach in order to obtain a reasonably accurate estimate of <n> and W_{kin}. In the previous work [1] the LIDAR data were not available for all the campaigns from 1984 to 1992, so the choice of the ECE and the DCN interferometer data as the basis for the W_{kin} estimate were mandatory. Now the LIDAR data are available for practically every selected time slice (758 cases out of 766) and have therefore been included in the present analysis.

Table 2. Averages of the ratios between LIDAR and ECE results for electron temperature measurements for the operation years.

	1994	**1995**	**1996**	**1994-96**
$T_{e0\ LIDAR/ECE}$	0.90±0.18	0.92±0.12	0.99±0.15	0.93±0.16
$\langle T_e \rangle_{LIDAR/ECE}$	0.90±0.13	0.97±0.10	1.13±0.13	0.99±0.16

The ECE and LIDAR T_e measurements are compared in Table 2 which lists the averages of the ratio of values measured by the two diagnostics for both T_{e0} and the volume averaged electron temperature $\langle T_e \rangle$. From Table 2 it can be concluded that the general agreement between the two diagnostic systems is very good. Nevertheless for the campaign 1994-1995 the LIDAR system did not observe the plasma centre. It was moved vertically to correct this

problem before the start of the 1996 campaign. It could be that the systematic enhancement of the LIDAR T_{e0} data for 1996 is due to this modification. Another element to take into account in the discussion of the T_e profile measurements is the observation made in the previous work [1] that JET ohmic data appear to respect the ohmic constraint [2] which reads $q_{cyl}^{2/3} < T_{e0}/\langle T_e \rangle < q_{cyl}$. This will be discussed further in the next section, but a plot analogous to Figures 3a,b using LIDAR instead of ECE data shows the same trends but with a much larger dispersion, so that a larger random error can be inferred. For all these reasons the ECE measurements are still preferred in this paper.

In order to assess and compare LIDAR density measurements and the DCN interferometer density measurements a reduced subset of the database has been selected which includes only the pulses for which the DCN data have been fully checked (88 time slices out of 766), as deduced by the status flag in the JET databases. In Table 3 the results of the two diagnostics are compared. The LIDAR estimates are systematically but only slightly lower than the DCN Abel inverted results. This is independent of the year of operation. Therefore the LIDAR data for $\langle n \rangle$ will be used in this paper to avoid the problem of the fringe jumps on the DCN results. However, the accuracy of the LIDAR density measurements depends on the accuracy of the LIDAR temperature results so only the time slices for which the ratio between LIDAR and ECE measurements of T_{e0} lies in the range defined by the first row of Table 2, for the year of interest, are included in the database.

Table 3: Averages of the ratios between LIDAR and DCN results for electron density measurement for the operation years.

	1994	**1995**	**1996**	**1994-96**
$n_{e0\ LIDAR/DCN}$	1.00±0.09	0.84±0.09	0.86±0.11	0.88±0.12
$\langle n_e \rangle_{LIDAR/DCN}$	0.88±0.09	0.84±0.06	0.85±0.10	0.85±0.09

In the JET databases there are two estimates of the kinetic electron energy content that are available for most pulses. The first, $W_{eECE+DCN}$, is based on the ECE and DCN data while the second, W_{eLIDAR}, is based only on the LIDAR results. Both these estimates can be compared with the plasma energy content W_{EFIT} as estimated by the equilibrium code EFIT. The precision of the diamagnetic estimate appears not to be sufficient in the case of the low values of W_{kin} typical of the ohmic plasma discharges and will not be considered here as in the previous paper [1]. In Table 4 the ratio between the different estimates of W_{kin} are shown for each year. The averages have been performed on the subset of the database for which all relevant data are available (717 out of 776). It can be concluded again that the agreement between the diagnostics is good. It can also be seen that the values of $W_{eECE+DCN}$ and those of W_{EFIT} are in good agreement independently of the year of operation, as the problem of fringe jumps probably affects more the error on the ratio instead of the ratio itself. It appears from Table 4 that the value of

W_{eLIDAR} is systematically about 20 % higher for 1996, compared to the previous two years. The reason for this is unclear, it could be a random effect or it could be correlated with the already mentioned modification of the LIDAR diagnostics before the 1996 campaign or with the related software. Therefore, in the present paper the estimate of the electron energy content will be based on $W_{eECE+DCN}$, but in order to minimise the effect of the undetected fringe jumps in the DCN measurements, data will only be retained if there is a good agreement between the density measurements from DCN and LIDAR. On the basis of the results in Table 3, the acceptance range for the ratio between the two measurements has been chosen to be 0.75-0.95.

Table 4: Averages of the ratios between the estimates of the plasma energy content.

	1994	**1995**	**1996**	**1994-96**
$W_{eLIDAR}/W_{eECE+DCN}$	0.97±0.14	1.00±0.12	1.21±0.14	1.05±0.17
$W_{EFIT}/2xW_{eECE+DCN}$	0.91±0.18	1.00±0.22	1.02±0.17	0.97±0.20
$W_{EFIT}/2xW_{eLIDAR}$	0.96±0.30	1.01±0.26	0.84±0.16	0.95±0.26

In order to reject time slices for which the current profile is still evolving the selection criterion $0.8 < V_{axis}/V_{sur} < 1.2$ has also been applied, as in the previous work [1].

The application of all the defined selection criteria results in a final database consisting of 80 time slices for limiter plasmas (from 71 pulses) and 299 time slices for diverted plasmas (from 186 pulses). Of the 80 limiter datasets only 11 are taken during the magnetic field ramp up.

In the evaluation of ion energy content from the experimental neutron yield two approaches as described in the previous paper [1] have been adopted. The first approach consists in fixing the Deuterium concentration to 0.5 and the resulting energy content and confinement time are labelled W_{kin1} and τ_{E1}, respectively. The second approach consists in fixing the main impurity species (Carbon) and evaluating the Deuterium concentration from the experimental value of the effective charge Z_{eff}. The resulting energy content and confinement time have been labelled W_{kin2} and τ_{E2}, respectively. The latter assumption appears to be more reasonable for the data of the present campaigns, especially for diverted plasmas, due to the low values of Z_{eff}. The first approach has been retained to permit an homogenous comparison with the results of the previous paper[1].

3. DATABASE DESCRIPTION AND ANALYSIS

The composition of the 1994-1996 ohmic database reflects the characteristic of the current JET operation in that the limiter subset is only 1/3 of the overall database, with a restricted density range and low current values compared to the 1984-1992 campaigns. Diverted data on the contrary reach much higher densities, especially for the MARK I divertor campaigns of 1994 and

1995. The bulk of the data consists of 2 MA discharges whereas it was 3 MA discharges for the 1984-1992 campaigns. The dataset for the MARK II divertor is at present limited to a large part of the 1996 campaign and constitutes a preliminary assessment of the present JET configuration.

The Z_{eff} values, as measured by visible bremsstrahlung, are comparable with the values obtained in the previous campaigns for the limiter plasma while the diverted plasma show a systematically lower value, especially during the MARK I operation. The radiated power fraction is correlated with the value of Z_{eff} at low density. Limiter plasmas have a radiated power fraction in the range 20-60%, while for divertor plasmas at the same density the range is 15-45%. At higher plasma density, where only divertor data are available the radiated fraction increases up to 70% at the maximum density values. Figures 1 a,b show the value of q_{cyl} versus B_T for the limiter and divertor plasmas, respectively. The parameter ranges for the limiter data are I_P (1-2.5) MA, B_T (1.6-3.5) T, q_{cyl} (2.3-7), κ(1.25-1.45) and for the divertor data I_P (2-3.5) MA,

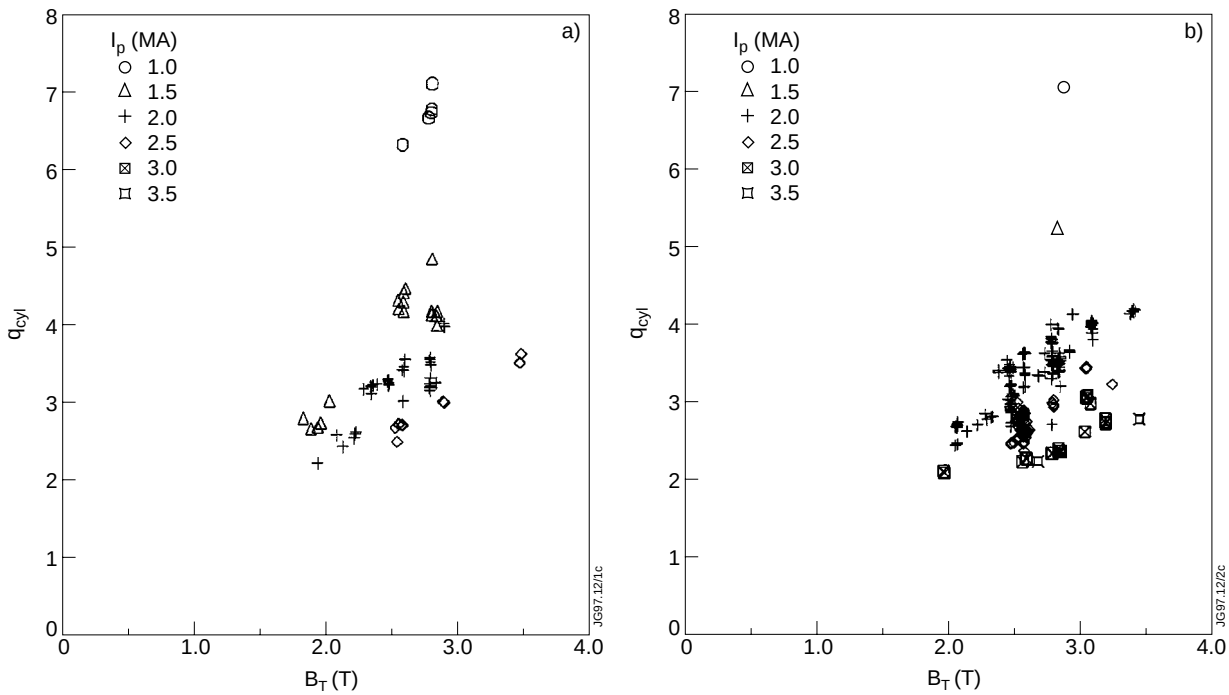

Fig.1. JET ohmic data from 1994-1996 campaigns: q_{cyl} versus B_T for a) limiter b) divertor plasma. The symbols refer to the plasma current values.

B_T (1.9-3.4) T, q_{cyl} (2.3-4.2), κ (1.5-1.8) with just a couple of cases at low current, high q_{cyl} values. Figures 2 a,b show the Hugill diagram for the limiter and divertor data, respectively. The limiter data are a factor of 2 below the Greenwald limit whereas some of the divertor data from the 1994 campaign reach this limit. As previously described in [1], the ohmic constraint on the T_e profiles[2] is well satisfied by JET plasma, as shown in Figures 3a,b for both limiter and

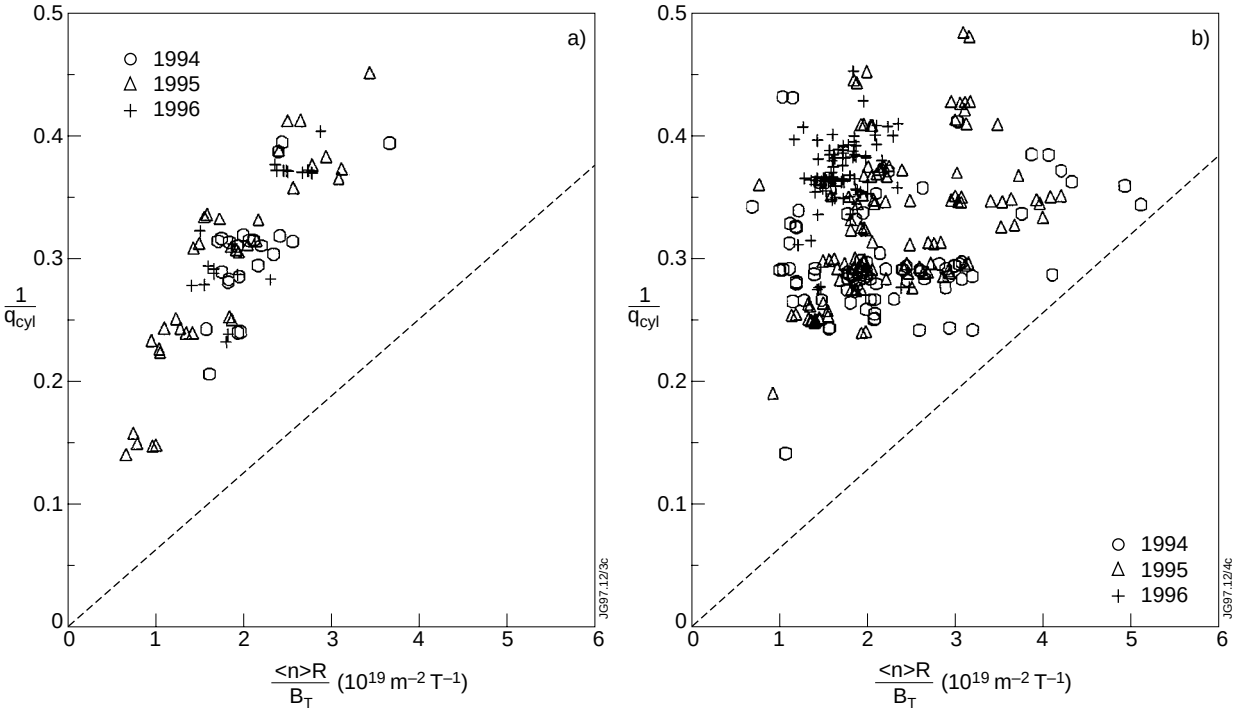

Fig.2. JET ohmic data from 1994-1996 campaigns: Hugill diagrams for a) limiter and b) divertor plasmas. The dotted line indicates the Greenwald limiter. The symbols refer to the operation year.

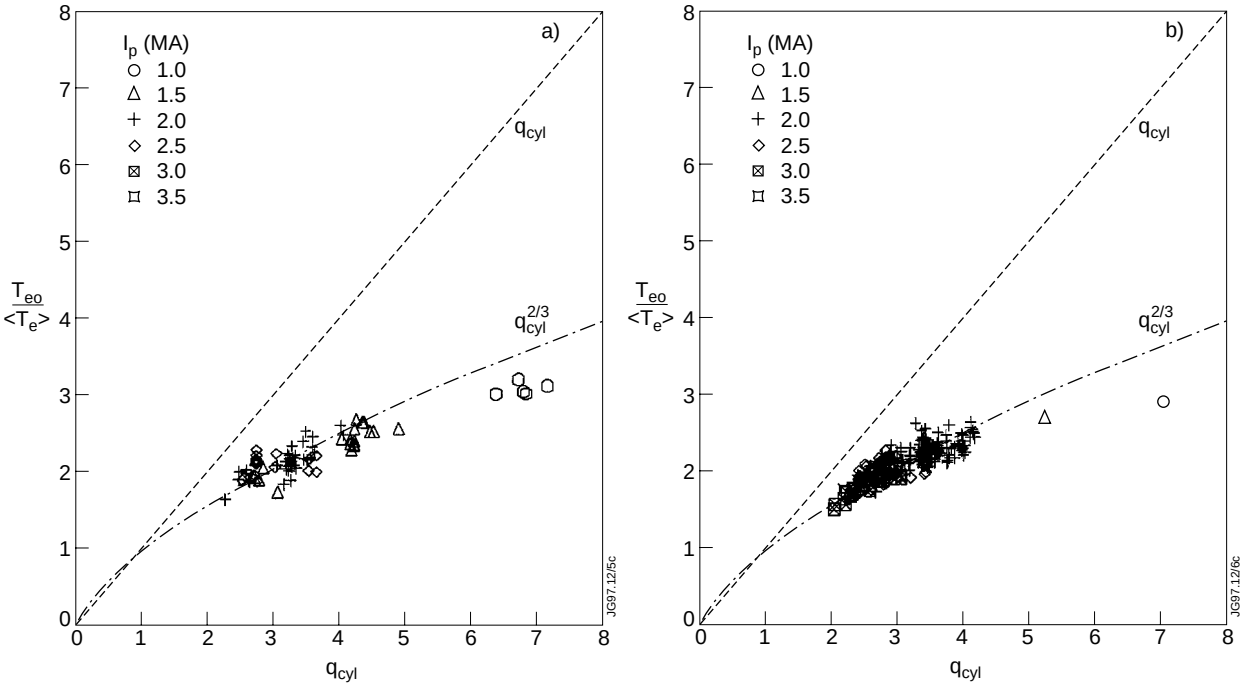

Fig.3. JET ohmic data from 1994-1996 campaigns: the peakedness of the electron temperature profile $T_{e0}/<T_e>$ is plotted versus q_{cyl} for a) limiter and b) divertor plasmas. The dotted lines corresponds to the ohmic constraints limits given by [2]. The symbols refer to the plasma current values.

divertor plasma. In figures 4 the values of τ_{E2} are shown versus volume averaged density for diverted plasma at 2 MA, 2.5 T, q_{cyl} = (2.7-3.7) that constitutes the richest subset of the database. It can be observed that no data are available at very low density, lower than 1x10^{19} m^{-3}, so that

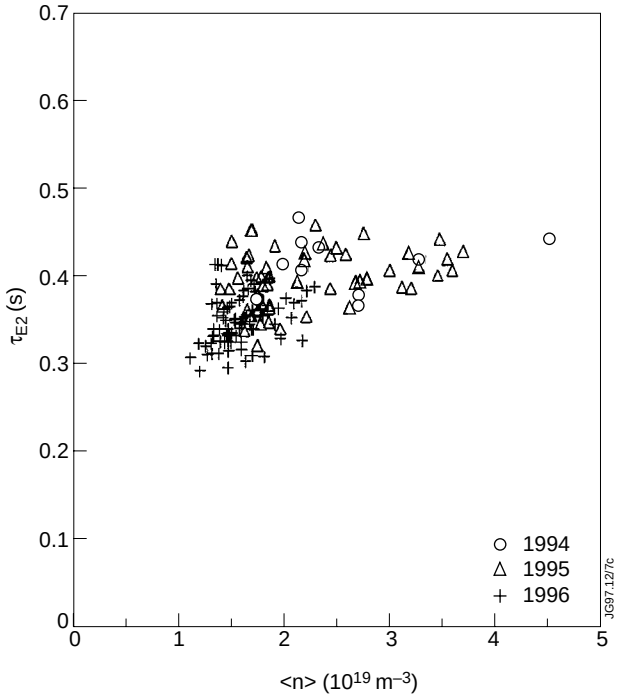

Fig.4. JET ohmic data from 1994-1996 campaigns: global energy confinement time versus the volume averaged density for diverted plasma at 2 MA, 2.5 T. The symbols refer to the operation year.

the linear dependence of the confinement time on density, typical of the linear ohmic confinement regime (LOC), can not be identified clearly. No systematic differences appear for data of the different years, but again the MARK II results from 1996 are restricted in a narrow density range. In figure 5 the previous data are compared to the limiter data with the same plasma parameters: the value of the confinement time appear to be the same in limiter and diverted plasma. The same conclusion can be drawn also from figure 6, where the confinement time for limiter and diverted plasma is shown as a function of <n>, for discharges at 2 MA, 2.8 T, q_{cyl}=(3-4). Limiter discharges have minor radius a_{min} in the range (0.95-1.05 m) and κ (1.25-1.45), while diverted plasma have a reduced minor radius a_{min} (0.85-1.0 m) and higher elongation κ (1.5-1.8). The apparent independence of energy confinement on elongation or configuration will be discussed in the following sections.

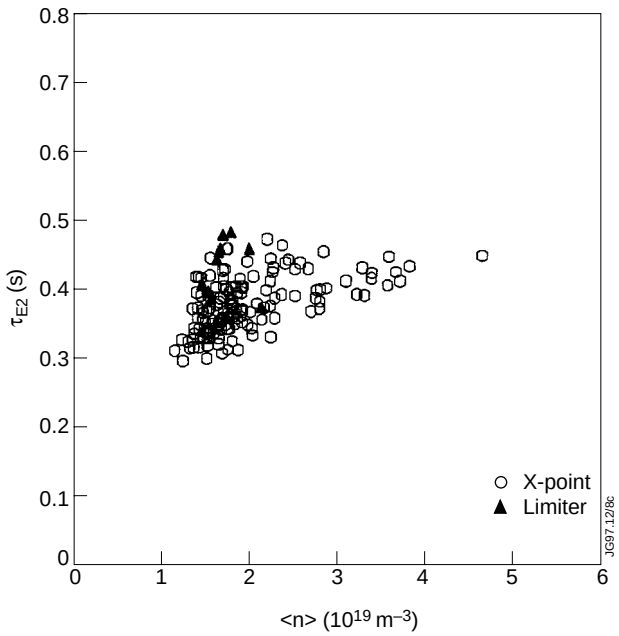

Fig.5. JET ohmic data from 1994-1996 campaigns: global energy confinement time versus the volume averaged density for plasma at 2 MA, 2.5 T. The symbols refer to limiter and divertor configurations.

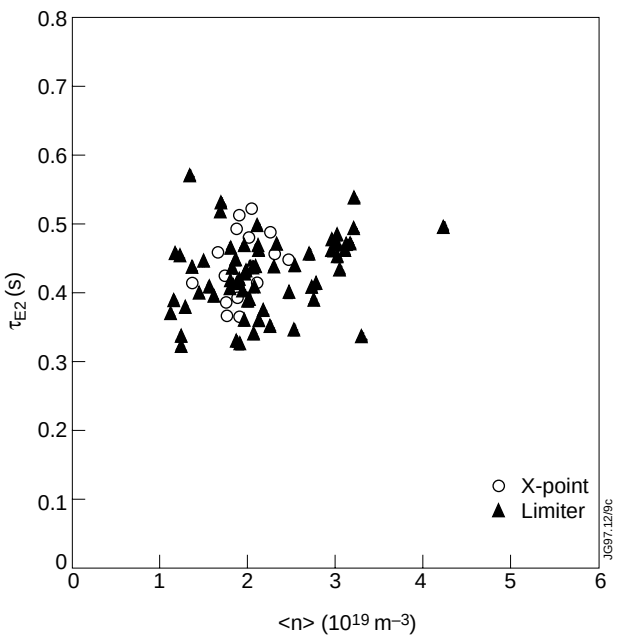

Fig.6. JET ohmic data from 1994-1996 campaigns: global energy confinement time versus the volume averaged density for plasma at 2 MA, 2.8 T. The symbols refer to limiter and divertor configurations.

4. COMPARISON WITH SCALING LAWS

In Figures 7a,b the confinement time for all the data in the database is shown versus the Neo-Alcator scaling (INTOR version) for limiter and diverted plasmas, respectively. The behaviour is similar to what was observed in [1]. In Figures 8a,b the same data are compared with

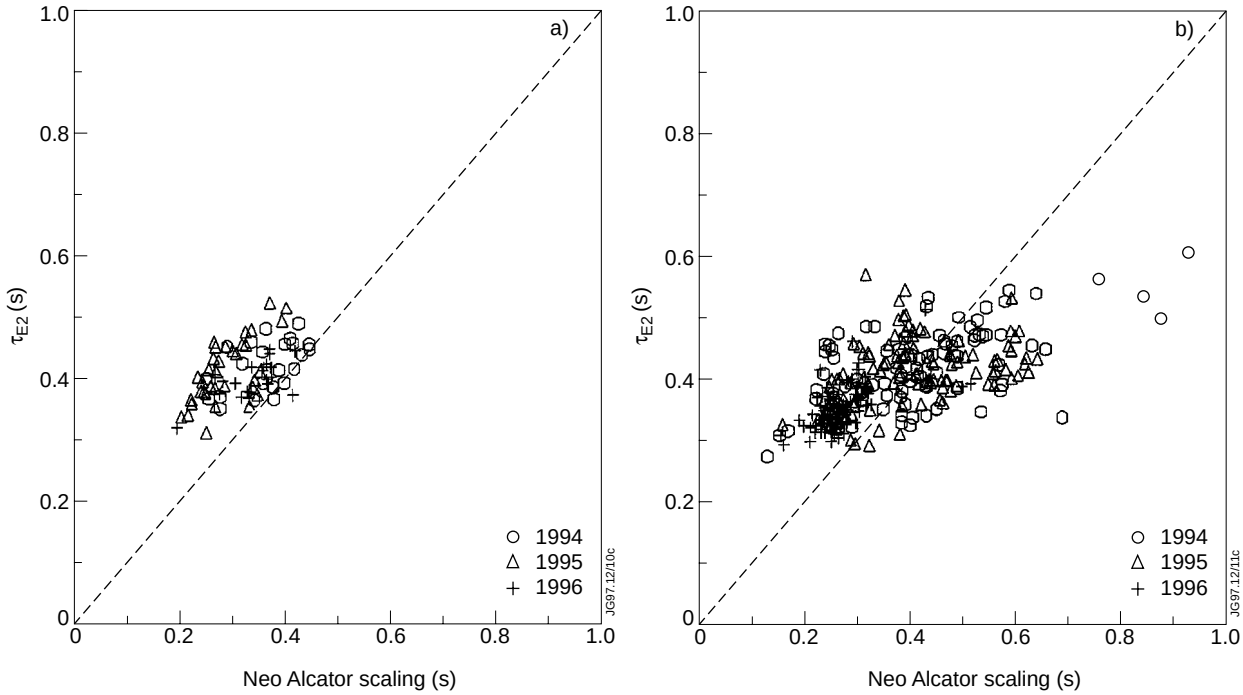

Fig.7. JET ohmic data from 1994-1996 campaigns: global energy confinement time versus Neo-Alcator scaling for a) limiter and b) divertor plasmas. The symbols refer to the operation year.

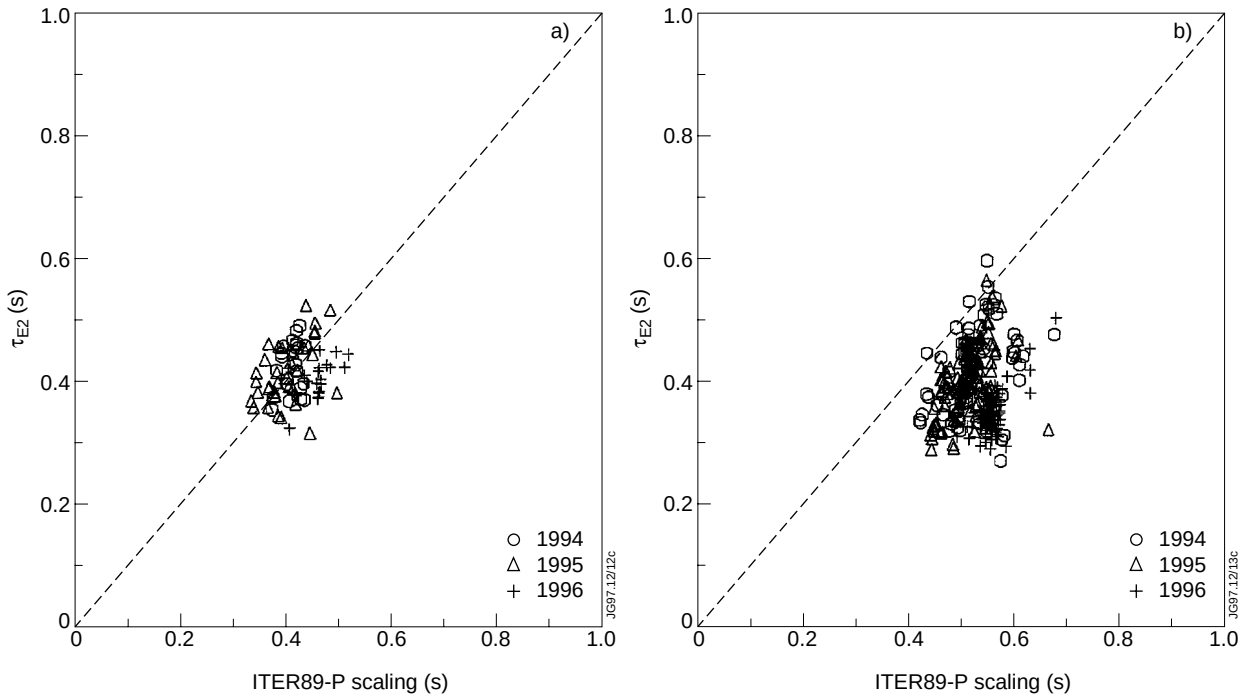

Fig.8. JET ohmic data from 1994-1996 campaigns: global energy confinement time versus ITER89-P scaling for a) limiter and b) divertor plasmas. The symbols refer to the operation year.

ITER89-P and again the situation appear to be similar to the past as it is illustrated in Figure 9, where the ratio between τ_{E2} and ITER89-P is shown versus <n>. The data appear to be in a better agreement with the scaling at high density values, deep in the saturated confinement regime (SOC). It can be noticed that there is a slight systematic dependence of the agreement on the value of the magnetic field. In Figures 10a,b the same data are compared with the Lackner-Gottardi scaling and in this case the limiter data appear to be in much better agreement than the divertor data. The discrepancies for the divertor data arise both from the almost linear dependence on κ and on the strong <n> dependence of this scaling law, as it can be observed in Figure 11, where the ratio between τ_{E2}. And the Lackner Gottardi scaling is shown versus <n>. At low density the disagreement is due essentially to the κ dependence, while the increasing discrepancy at higher density is due to the <n> dependence in the scaling.

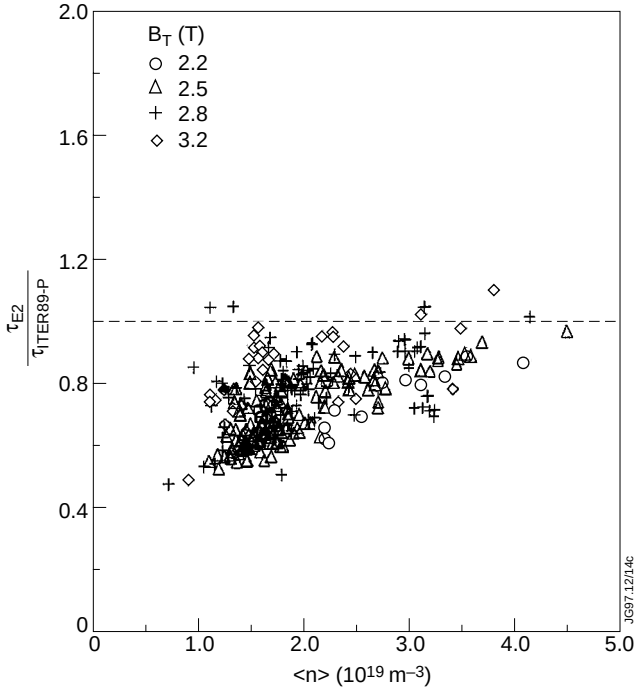

Fig.9. JET ohmic data from 1994-1996 campaigns: ratio between the global energy confinement time and ITER89-P scaling versus volume averaged density for divertor plasmas. The symbols refer to the magnetic field value.

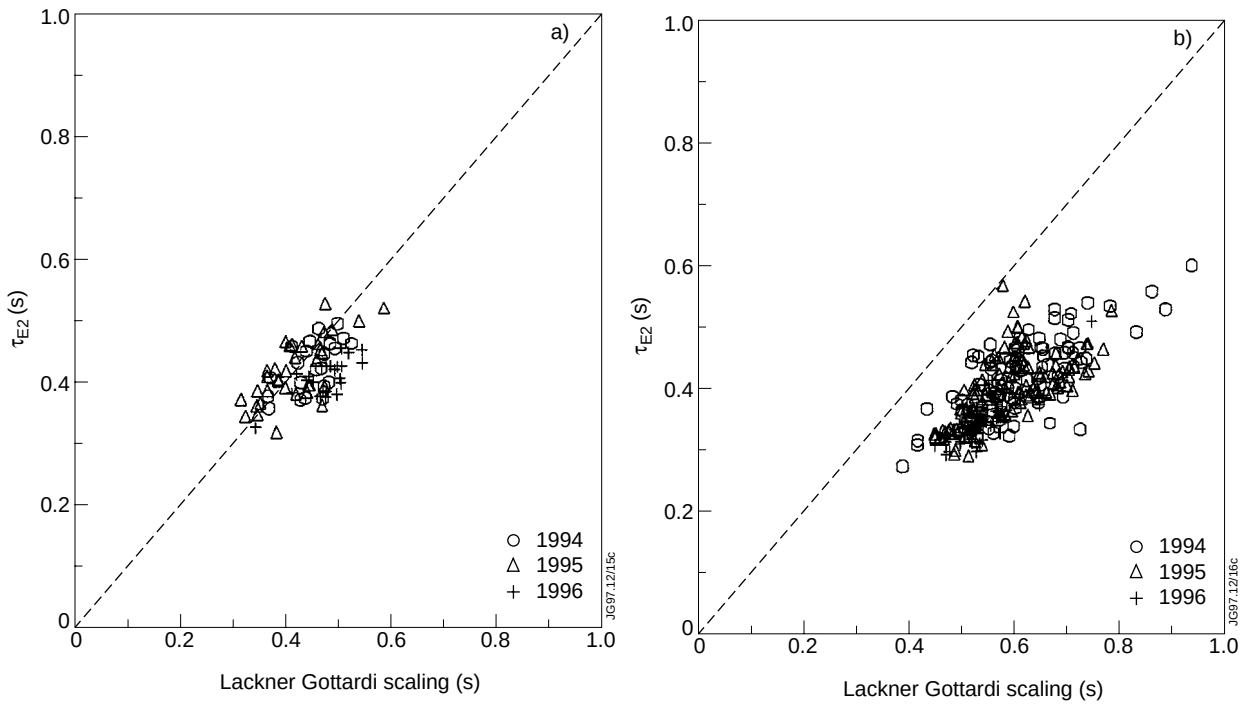

Fig.10. JET ohmic data from 1994-1996 campaigns: global energy confinement time versus Lackner-Gottardi scaling for a) limiter and b) divertor plasmas. The symbols refer to the operation year.

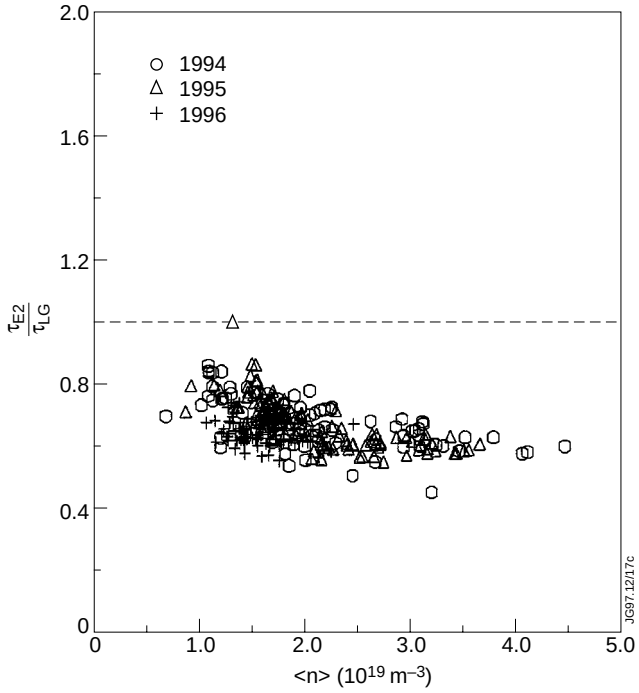

Fig.11. JET ohmic data from 1994-1996 campaigns: ratio between the global energy confinement time and Lackner-Gottardi scaling versus volume averaged density for divertor plasmas. The symbols refer to the operation year.

5. ANALYSIS OF SATURATED CONFINEMENT REGIME

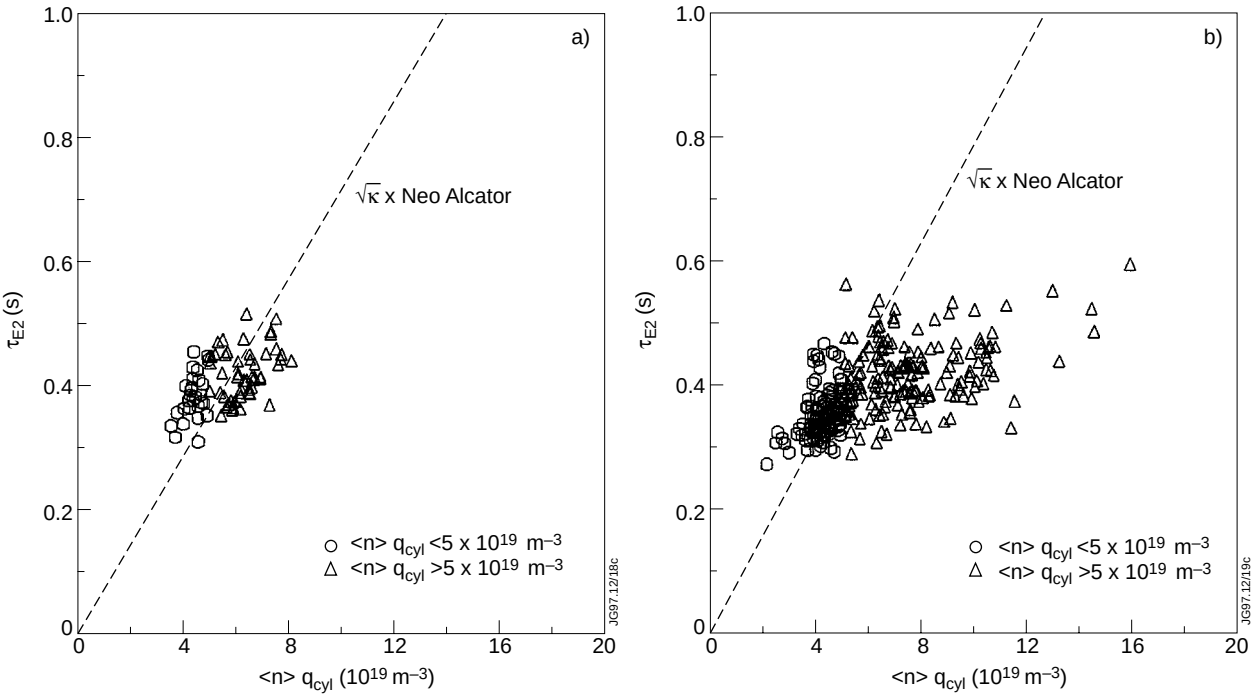

Fig.12. JET ohmic data from 1994-1996 campaigns: global energy confinement time versus <n> q_{cyl} for a) limiter b) divertor plasma. Data below and above the definition of the SOC regime provided in [1] are marked with different symbols.

As it has been noticed in [1] the B_T dependence of the global confinement time in the saturated ohmic regime can be connected to the plasma size dependence by means of the Connor-Taylor constraints. Figures 12a,b show τ_{E2}. versus $\langle n \rangle q_{cyl}$. In [1] the SOC regime had been identified with plasmas having $\langle n \rangle q_{cyl} > 5x10^{19}$ m^{-3}. The results of the present work show a very limited amount of data above that threshold for limiter plasma, so that no conclusion can be drawn. However, the diverted plasma data are mostly in the SOC regime.

If a B_T regression is performed on the divertor data the result is $\tau_{E2} \approx B_T^{0.80\pm0.07}$ (correlation coefficient 0.67).This dependence is slightly higher that the one found in the previous work, $\tau_{E2} \approx B_T^{0.66}$, but the stronger B_T dependence of JET data compared to that of smaller tokamaks is now confirmed by the 1994-1996 campaigns. Figure 13 shows the values of τ_{E2} versus $\langle n \rangle$ for diverted plasma at 2 MA, and the rather strong B_T dependence can clearly be observed. If the regression of the SOC data only is performed by including also κ, $\langle n \rangle$ and I_P, the following result is obtained: $\tau_{E2} \approx B_T^{0.90\pm0.07} \langle n \rangle^{0.35\pm0.03} \kappa^{0.27\pm0.20} I_P^{-0.22\pm0.06}$. The correlation coefficient is only slightly higher, 0.67, but it can be noticed that even if the magnetic field dependence is definitely the strongest, some residual dependence on density can be identified, as also observed in Figure 13. In Table 5 the correlation coefficients for the quantities involved in the regressions are shown, and no strong correlation can be identified. The table also includes Z_{eff} that has been excluded from the regression as its exponent is very close to zero.

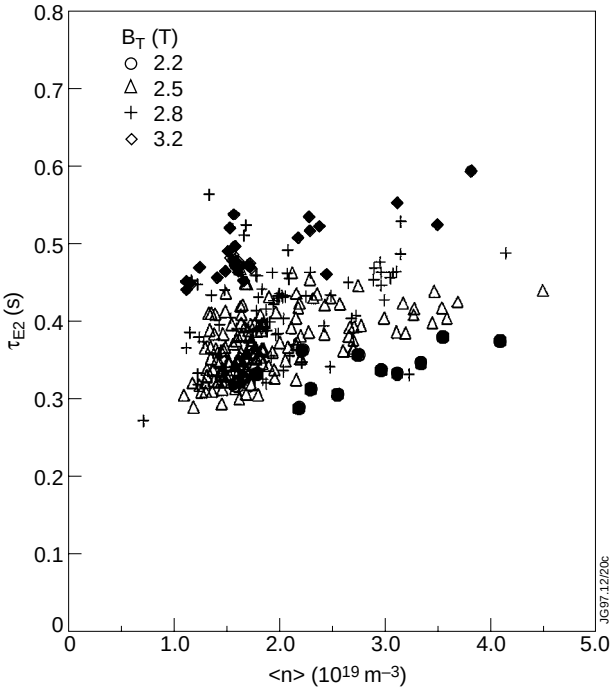

Fig.13. JET ohmic data from 1994-1996 campaigns: global energy confinement time versus volume averaged density for divertor plasmas at 2 MA. The symbols refer to the magnetic field value.

Table 5: Correlation coefficients for divertor data in SOC regime.

	κ	B_T	I_P	$\langle n \rangle$	Z_{eff}
κ	1				
B_T	-0.398	1			
I_P	0.145	0.156	1		
$\langle n \rangle$	0.359	-0.167	0.310	1	
Z_{eff}	0.002	-.036	0.071	-0.208	1

6. COMPARISON WITH DATA FROM 1984 TO 1992

The comparison between the present results from the years 1994-1996 and those from the years1984-1992 must take into account the change in the JET device and the operation scenarios. Most of the old data are for limiter plasma, while the present results are mostly with a divertor configuration. The plasma volume in JET is approximately 30% smaller with the MARK I divertor installed than without and it has been only marginally increased with the installation of the MARK II divertor, as shown in Table 6:

Table 6. Average value of the plasma volume for the old campaigns and the recent ones, where the average is performed on the data of the ohmic databases.

Operation years	Average plasma volume (m^3)
1984-92	115±5
1994 MARK I	75.1±4.5
1995 MARKI	75.3±5.5
1996 MARK II	79.4±5.0

Limiter and diverted plasmas appear to have similar plasma volumes, as the reduced minor radius is compensated by the increased elongation.

The results of the regressions on the 1984-1992 data [1] are listed in Table 7 because they are used in the comparison and in [1] the normalisation coefficients were not provided.

Table 7. Exponents and coefficients of the regressions for the main confinement quantities for the Deuterium, limiter data of the 1984-1992 database.

	C_0	I_P (MA)	$\langle n \rangle$ ($10^{19}m^{-3}$)	B_T (T)
$\langle T_e \rangle$ (keV)	0.434	1.01	-0.57	0.22
W_e (MJ)	0.159	0.90	0.47	0.33
W_{kin} (MJ)	0.231	0.80	0.60	0.36
V_{sur} (V)	0.798	0.20	0.22	-0.38
τ_E (s)	0.284	-0.40	0.39	0.79
T_{e0} (keV)	1.022	0.40	-0.50	0.79
	C_0	Z_{eff}	$\langle n \rangle$ ($10^{19}m^{-3}$)	B_T (T)
V_{sur} (V)	0.754	0.24	0.39	-0.41
T_{e0} (keV)	1.081	0.23	-0.29	0.91

Table 8. Averages, standard deviations, minima and maxima of the ratio between the confinement related quantities and the corresponding regressions obtained on previous JET campaigns, Table 6, both for limiter and diverted plasma discharges.

Limiter Plasma	**Mean**	**Standard Deviation**	**Minimum**	**Maximum**
$<T_e>$/Regr.	1.332	0.174	1.049	1.717
W_e/Regr.	0.689	0.089	0.513	0.924
W_{kin1}/Regr.	0.680	0.072	0.511	0.814
W_{kin2}/Regr.	0.728	0.073	0.559	0.870
V_{sur}/Regr.	0.992	0.101	0.798	1.234
τ_{E1}/Regr.	0.678	0.075	0.535	0.842
τ_{E2}/Regr.	0.727	0.083	0.583	0.924
V_{sur}/Regr.(Z_{eff})	0.960	0.099	0.764	1.218
T_{e0}/Regr.	1.024	0.092	0.828	1.220
T_{e0}/Regr.(Z_{eff})	0.860	0.078	0.677	1.006
X-POINT Plasma				
$<T_e>$/Regr.	1.112	0.096	0.865	1.371
W_e/Regr.	0.543	0.053	0.388	0.689
W_{kin1}/Regr.	0.544	0.046	0.396	0.744
W_{kin2}/Regr.	0.598	0.048	0.442	0.863
V_{sur}/Regr.	0.836	0.065	0.653	1.013
τ_{E1}/Regr.	0.635	0.082	0.386	0.917
τ_{E2}/Regr.	0.697	0.085	0.430	1.063
V_{sur}/Regr.(Z_{eff})	0.882	0.075	0.671	1.223
T_{e0}/Regr.	0.906	0.058	0.768	1.107
T_{e0}/Regr.(Z_{eff})	0.849	0.076	0.623	1.099

In Table 8 the averages of the ratio between the main confinement related quantities and the corresponding regressions on the 1984-1992 data are shown, together with their standard deviations and the variation ranges. For some of the data the plot of the present data versus the 1984-1992 regression are also shown: in Figure 14a,b the regression of $<T_e>$, in Figure 15a,b the

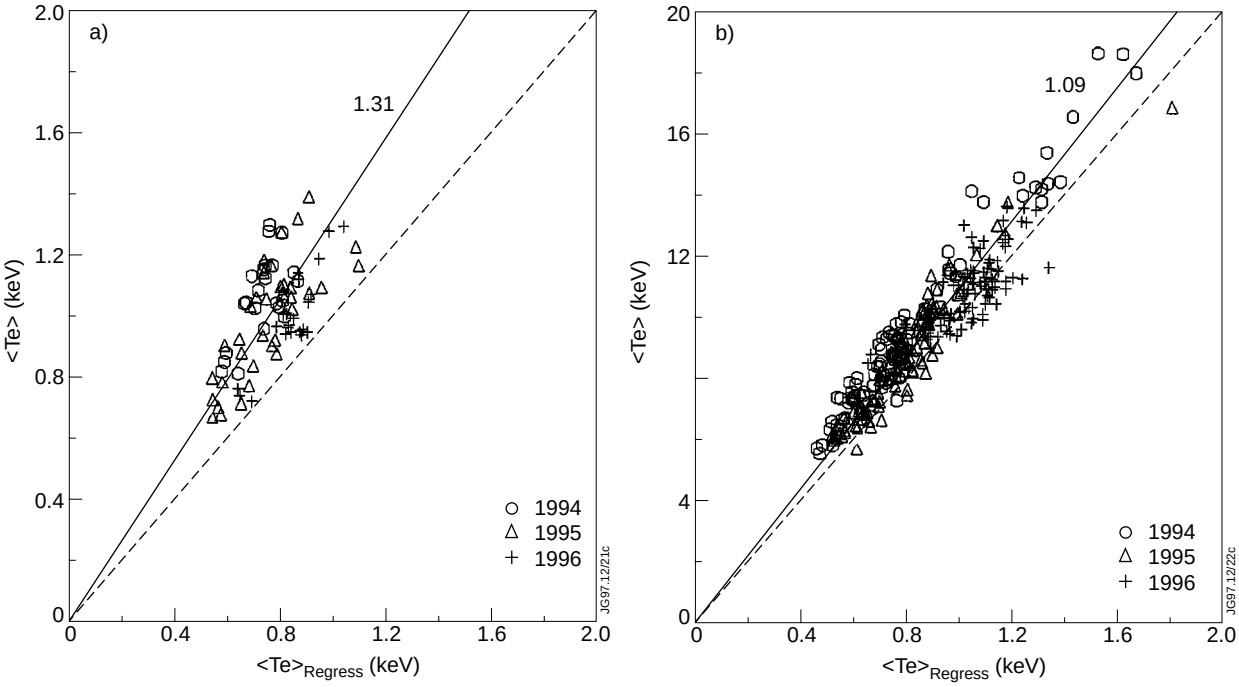

Fig.14. JET ohmic data from 1994-1996 campaigns: $<T_e>$ versus the corresponding 1984-1992 regression with I_P, <n> and B_T, Table 7, for a) limiter b) divertor plasma. The full line indicates the best fit. The symbols refer to the operation year.

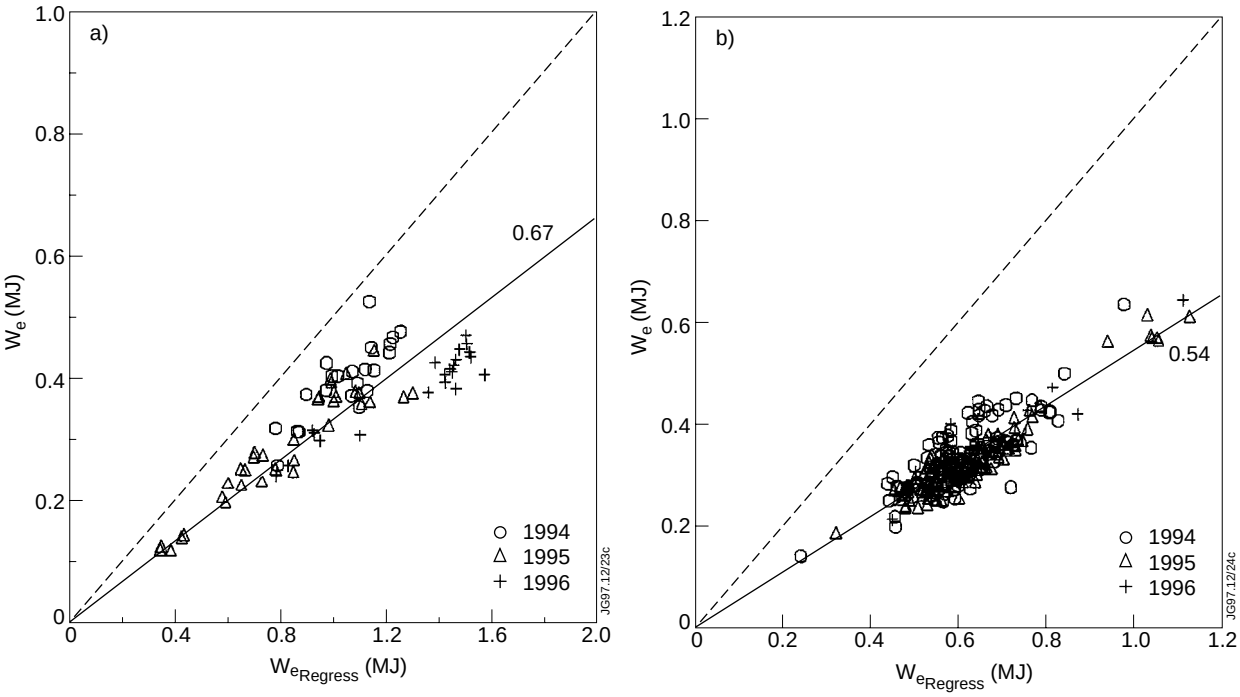

Fig.15. JET ohmic data from 1994-1996 campaigns: W_e versus the corresponding 1984-1992 regression with I_P, <n> and B_T, Table 7, for a) limiter b) divertor plasma. The full line indicates the best fit. The symbols refer to the operation year.

regression of W_e, in Figure 16a,b the regression for V_{sur} and in Figure 17a,b the regression for T_{e0}, where the index a and b refer to limiter and diverted plasma configurations. As the regressions were performed on the limiter subset of the 1984-1992 database the comparison with the

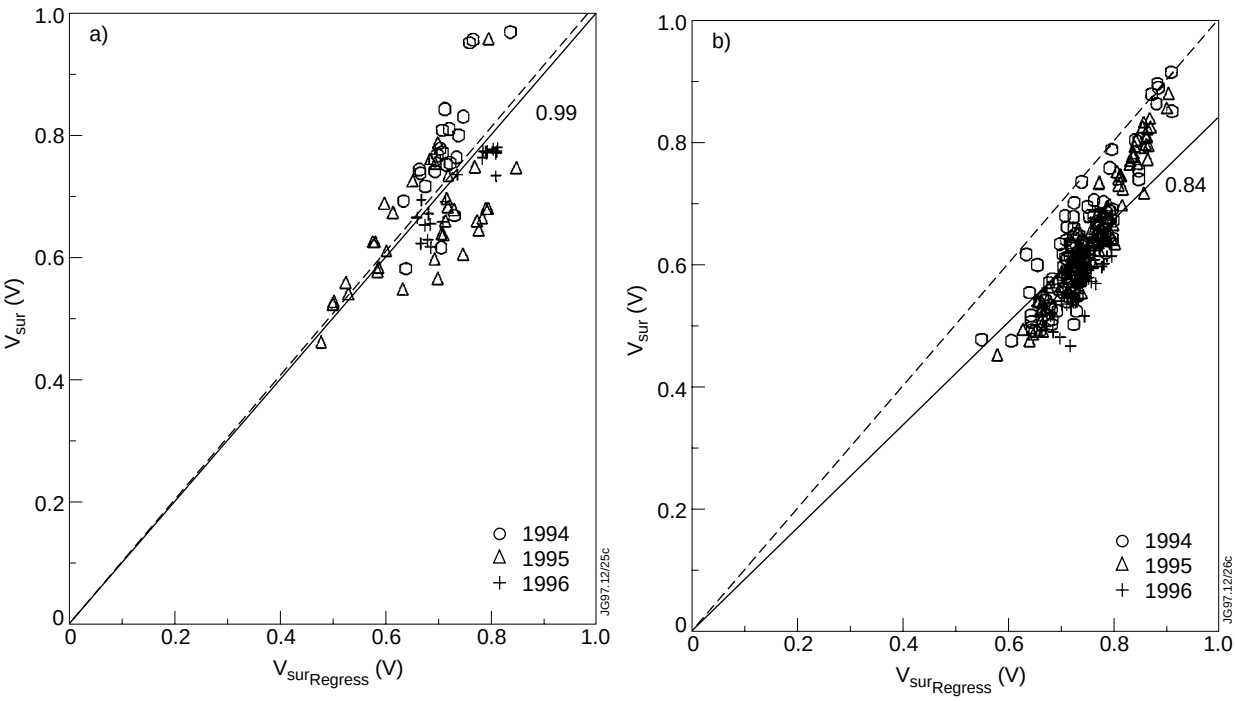

Fig.16. JET ohmic data from 1994-1996 campaigns: V_{sur} versus the corresponding 1984-1992 regression with I_P, <n> and B_T, Table 7, for a) limiter b) divertor plasma. The full line indicates the best fit. The symbols refer to the operation year.

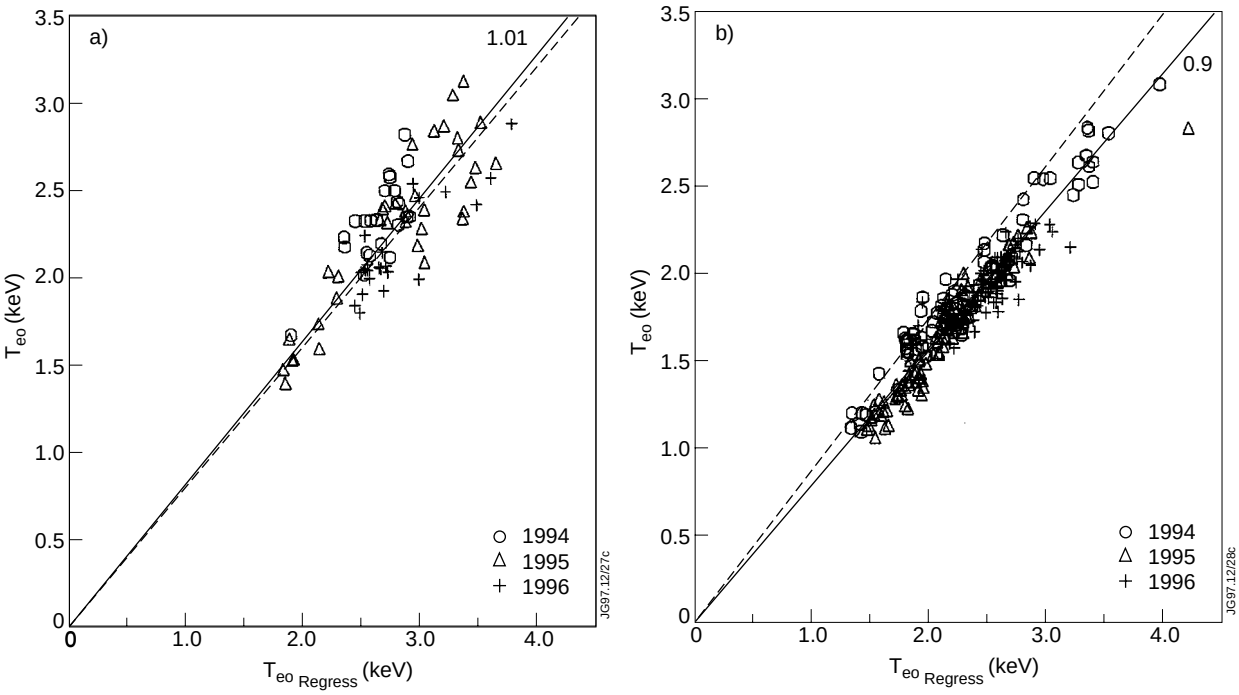

Fig.17. JET ohmic data from 1994-1996 campaigns: T_{e0} versus the corresponding 1984-1992 regression with I_P, <n> and B_T, Table 7, for a) limiter b) divertor plasma. The full line indicates the best fit. The symbols refer to the operation year.

present limiter data is more relevant, as also the values of Z_{eff} appear to be similar. From Table 8 the comparison can be summarised as follows: at the same value of I_P, <n> and B_T the recent data have the same value of V_{sur} and T_{e0} as the old database, the value of $<T_e>$ is increased

30% due to the reduction in the plasma volume, while W_e , W_{kin} and consequently τ_E are reduced by the same factor. The two different approaches to estimate the ion energy content that have led to the definition of W_{kin1}, τ_{E1} and W_{kin2}, τ_{E2}, respectively, do not have an relevant effect on the previous observations, as it can be concluded from examining the values reported in Table 8. The underlying reason for the dependence of the present scaling of the main confinement data with the size of the plasma cross-section is unclear, but the comparison between the two databases provides a clear picture of the experimental evidence. If the divertor data are considered, the bulk of the previous considerations can be maintained, but the effect of different Z_{eff} values could play a relevant role. In fact the regression of V_{sur} as dependent on I_P, <n> and B_T does not appear to match nicely the divertor data while if the regression formula includes Z_{eff} instead of I_P a much better agreement is found, see Figure 18. From all the Figures 14-18 it can be also concluded that the MARK I and the MARK II data appear to have similar behaviour, without any systematic trend.

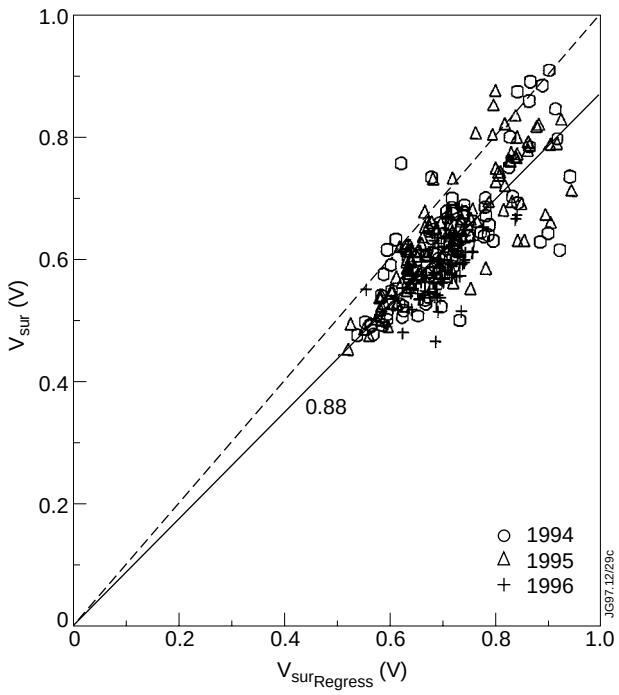

Fig.18. JET ohmic data from 1994-1996 campaigns: V_{sur} versus the corresponding 1984-1992 regression with Z_{eff}, <n> and B_T, Table 7, for divertor plasma. The full line indicates the best fit. The symbols refer to the operation year.

The comparison between limiter and divertor plasma in the campaigns 1984-1992, had shown some unclear features, reported in the previous paper [1]: most of the older divertor data had higher τ_E values compared to the limiter plasma with the same I_P, <n> and B_T , so that a dependence of the confinement with the square root of the elongation was inferred. Only a restricted subset of divertor data, obtained in the last years covered by the old database, showed a lower value of τ_E , much closer to the limiter data. No trivial explanation had been found for this feature, that was again correlated with a period of operation where the Z_{eff} was lower than usual for diverted plasmas. The fact that in the present situation, when divertor plasma have a systematic lower value of $Z_{eff,}$ the value of τ_E appear to be independent of the elongation, may suggest that the intrinsic elongation dependence of the global confinement on elongation is really lower than what expected and somewhat masked by an unclear dependence on the value of $Z_{eff.}$

VII. CONCLUSIONS

The analysis of the global energy confinement for the ohmic data obtained in the 1994,1995 and 1996 campaigns can be summarised as follows. The overall picture of the JET ohmic confinement as presented in the previous paper[1] has been confirmed. The choice of the diagnostics used to evaluate the plasma kinetic energy content has been adapted to the new situation of the available data. Due to the present operation scenarios, the database subset at very low density is very poor, so that the LOC regime can not be clearly identified. It can not be excluded that the present criteria for the data selection could be improved to enrich the database in that direction also, by examining for example the ohmic phase of the additional heated plasma discharges. If the present results are compared to the results obtained in the old campaigns 1984-1992, it can be concluded that the reduction in plasma volume, due to the introduction of the divertor, has reduced the value of the confinement time in the same proportion. The energy transport in the plasma seems to have adapted itself so that the peak electron temperature and the loop voltage have not been changed by the reduction of the volume. Between the MARK I and the MARK II divertor configurations no strong difference in global energy confinement can be detected. It can be observed that the latter configuration has apparently reduced the available density range at least in the part of the MARK II campaign completed up to the time of this analysis (end of November 1996). The dependence of the global confinement on κ is still unclear as it appears that the dependencies on elongation, configuration and Z_{eff} are not independent in the operation scenarios and the resulting database.

REFERENCES

[1] BRACCO, G., THOMSEN, K., Nuclear Fusion 37 (1997) 759.

[2] WALTZ, R. E., et al., Nuclear Fusion 26 (1986) 1729.